3 Spatial Modeling

Pablo A. Iglesias

Many, if not most, of the mathematical models in cell biology assume a homogeneous spatial distribution of the biochemical entities involved. This assumption facilitates the use of ordinary differential equations to describe the reactions governing the species concentrations. In practice, however, cells are not well-stirred biochemical reactors where proteins and other species are uniformly distributed. Instead, they consist of highly complex environments in which species are segregated to different spatial domains. In many cases, the spatial arrangement and regulation are as important to cellular function as the temporal behavior. For example, spatial segregation is crucial during development, giving rise to polarity in cells and, subsequently, in organisms. This chapter shows how spatial models in biology arise; it also presents some important properties regarding the control of spatial heterogeneities in cell biology.

3.1 Spatial Heterogeneities in Biological Models

Implicit in any ordinary-differential-equation (ODE) model of biological systems is the assumption that chemical concentrations are spatially homogeneous. This assumption is valid for systems in which the reactions are confined to small volumes or when the mobility of the interacting chemical species is restricted. In many systems, however, spatial heterogeneities are present and are important for proper cell function. Specifically, diffusion and transport of biochemical molecules can play a significant role in biological regulation.

This spatial segregation can be treated with compartment models, in which different parts of the cells are modeled separately using ODEs and transport between the compartments is incorporated. A good example of this type of model is found in Görlich et al. (2003), in which the cytoplasm and nucleus are modeled as well-stirred compartments and transport through the nuclear pore complexes is modeled explicitly.

Alternatively, partial-differential-equation (PDE) models can be used. In these models, systems of differential equations of the form

$$\frac{dc_i(t)}{dt} = f_i(c_1, \ldots, c_n),$$

where the f_i refer to the reaction terms, are replaced by equations that depend on both time, t, and spatial location, x. This can be inside a domain, Ω, or on the domain's boundary, $\partial\Omega$. The former can represent the cytoplasm, nucleus, or some other intracellular compartment; the latter can be, for example, the plasma membrane or nuclear envelope.

Taking transport into account, the concentration of species i obeys

$$\frac{\partial c_i(\boldsymbol{x}, t)}{\partial t} = -\nabla J_i(\boldsymbol{x}, t) + f_i(c_1(\boldsymbol{x}, t), \ldots, c_n(\boldsymbol{x}, t)). \tag{3.1}$$

In this equation, the function $J_i(\boldsymbol{x}, t)$ specifies the flux of molecules of species c_i into an infinitesimal volume at spatial location $\boldsymbol{x}$. It has units of molecules per unit area per unit time. The differential operator ∇ depends on the spatial dimension and the representation (Cartesian, polar, etc.) used to describe it. For simplicity, we mostly assume one-dimensional systems in this chapter, in which case $\nabla = \partial/\partial x$. The general principles presented here apply to more realistic spatial domains.

3.1.1 Diffusion

There are several ways in which molecular flux can arise. We first consider diffusion, the random motion of a molecules from areas of high concentration to areas of low concentration. Arising from the Brownian motion of individual molecules, diffusion can be described statistically on a microscale (Berg, 1993). Instead, we will employ a macroscale description based on Fick's law of diffusion, which states that the flux of a species into a region is proportional to the concentration gradient:

$$J_i(\boldsymbol{x}, t) = -D_i(\boldsymbol{x})\nabla c_i(\boldsymbol{x}, t). \tag{3.2}$$

The proportionality constant $D_i(\boldsymbol{x})$ is known as the *diffusion coefficient*. In general, it can depend on the location in the domain. The "$-$" sign is used since diffusion takes molecules from regions of higher concentration into regions of lower concentration. If we substitute equation (3.2) into equation (3.1), we get

$$\frac{\partial c_i(\boldsymbol{x}, t)}{\partial t} = \nabla(D_i(\boldsymbol{x})\nabla c_i(\boldsymbol{x}, t)) + f_i(c_1(\boldsymbol{x}, t), \ldots, c_n(\boldsymbol{x}, t)). \tag{3.3}$$

It is common to assume that diffusion is homogeneous—that is, independent of the spatial variable—in which case equation (3.3) simplifies to

$$\frac{\partial c_i(\boldsymbol{x}, t)}{\partial t} = D_i\nabla^2 c_i(\boldsymbol{x}, t) + f_i(c_1(\boldsymbol{x}, t), \ldots, c_n(\boldsymbol{x}, t)). \tag{3.4}$$

3.1.2 Transport

Diffusion represents passive transport. Biochemical species inside cells also move because of active transport processes. For example, actin or microtubule motors carry cargo along these polarized filaments in different directions (Bray, 2000). To model this transport, we will use the advection equation

$$J_i(\boldsymbol{x}, t) = v_i(\boldsymbol{x})c_i(\boldsymbol{x}, t), \tag{3.5}$$

where $v_i(\boldsymbol{x})$ is the velocity of the particles of species i. This velocity may depend on the spatial location $\boldsymbol{x}$.

3.1.3 Boundary Conditions

When specifying an ordinary differential equation, one must define the initial condition. For partial differential equations, one must also specify *boundary conditions*. Three types of boundary conditions are commonly used in models of biochemical reactions. We will assume that the partial differential equation is defined in the domain Ω with boundary $\partial\Omega$. For Dirichlet boundary conditions, the first type, the values of the concentration are fixed:

$$c_i(\boldsymbol{x}, t) = c_{0,i}(\boldsymbol{x}), \qquad \boldsymbol{x} \in \partial\Omega.$$

In practice, a more common situation in biological systems is to specify the flux of the species at the boundaries. For Neumann boundary conditions, the second type, the equation

$$\nabla c_i(\boldsymbol{x}) \cdot \vec{\mathbf{n}} = g_i(c_1(\boldsymbol{x}, t), \ldots, c_n(\boldsymbol{x}, t)), \qquad \boldsymbol{x} \in \partial\Omega,$$

specifies the boundary conditions, where $\vec{\mathbf{n}}$ is the outward normal direction to $\partial\Omega$.

The third type, Robin boundary conditions, arises as a linear combination of the first and second types:

$$k_1 c_i(\boldsymbol{x}) + k_2\nabla c_i(\boldsymbol{x}) \cdot \vec{\mathbf{n}} = g_i(c_1(\boldsymbol{x}, t), \ldots, c_n(\boldsymbol{x}, t)), \qquad \boldsymbol{x} \in \partial\Omega.$$

The functions g_i that arise in Neumann and Robin boundary conditions can include reactions that take place on the boundary, for example, reactions of membrane-bound particles that drive intracellular dynamics.

3.1.4 The Diffusion Equation

When there are no reaction terms, the partial differential equation reduces to the diffusion equation, which is also known as the heat equation. In one dimension:

$$\frac{\partial c(x,t)}{\partial t} = D\frac{\partial^2 c(x,t)}{\partial x^2}. \tag{3.6}$$

In a specific case that proves to be useful, the species diffuses in an infinite medium: $x \in (-\infty, \infty)$, and all the molecules are initially at the origin:

$$c(x,0) = c_0\delta(x),$$

where $\delta(x)$ refers to the Dirac delta function and the boundary conditions are such that $\lim_{x\to\infty} c(\pm x, t) < \infty$. Although the solution can be obtained in a straightforward manner using the method of *separation of variables* (Haberman, 1983), it is easier just to verify that

$$c(x,t) = \frac{c_0}{\sqrt{4\pi Dt}} e^{-x^2/(4Dt)} \tag{3.7}$$

satisfies equation (3.6). The profile of $c(x,t)$ in equation (3.7) is clearly that of a Gaussian curve with mean zero and variance $2Dt$. We can view this as the probability that a particle, initially at the origin, will have moved a distance x in time t seconds. In particular, we can get the mean square displacement:

$$\langle x^2 \rangle = \int_{-\infty}^{\infty} x^2 c(x,t)\, dx = 2Dt, \tag{3.8}$$

directly from the fact that equation (3.7) specifies a Gaussian distribution.

3.2 Morphogen Gradients

All biological systems exhibit spatial polarity at some point or another. In fact, even spherical bacteria (known as *cocci*) develop spatial asymmetry at the time of division (Cabeen and Jacobs-Wagner, 2007). How biological species polarize is one of the great questions in cellular and developmental biology (Arkowitz and Iglesias, 2008).

In developmental biology, morphogen gradients are believed to effect differentiation. A morphogen is a diffusible molecule that is produced or secreted at one end of an organism. Diffusion away from the localized source forms a gradient of concentration. This spatial pattern then controls the activity of downstream effectors, which may be other signaling molecules or other cells. Because the response of these effectors depends on the local concentration of the morphogen, which itself depends on the position, different cells along the length of the gradient experiencing different concentrations yield different responses (figure 3.1). The idea that gradients of diffusible particles could effect spatial patterns is about 100 years old (Ephrussi and St Johnston, 2004). Nobelist Thomas Hunt Morgan (1901) proposed that gradients

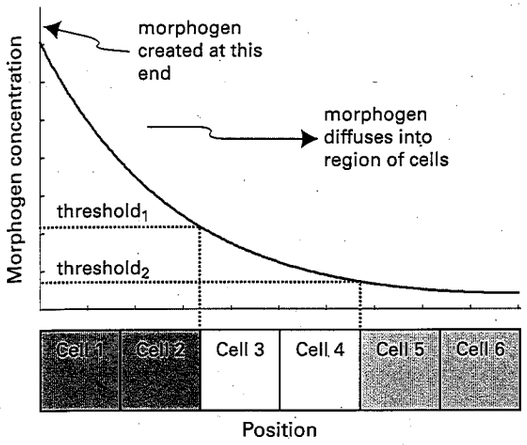

Figure 3.1
Morphogen gradients and the French flag model. A morphogen is secreted at the left end of a domain and diffuses into the area, where it is degraded or deactivated, creating a spatial gradient. The morphogen triggers downstream effectors in a concentration-dependent manner. In this example, the six cells exhibit three distinct phenotypes, depending on whether the morphogen concentration is above one or both of the thresholds. The resemblance of the resultant pattern to the French tricolor gives this model its name (Wolpert, 1969).

could be responsible for regeneration. That same year, Theodor Boveri (1901) suggested that the patterns in sea urchin larvae could be achieved by gradients.

The concept of morphogen gradients as a means of controlling spatial patterning and positional information during development was particularly championed by Lewis Wolpert (1969), who developed the so-called French flag model (figure 3.1). The existence of morphogens and their role in development have now been established experimentally; the first morphogen discovered was the transcription factor bicoid, in the fruit fly *Drosophila melagonaster* (Driever and Nüsslein-Volhard, 1988).

3.2.1 A Simple One-Dimensional Model

To see how a morphogen gradient can arise, we consider the case of a system consisting of a single species, whose concentration is denoted by $c(x,t)$, diffusing in a one-dimensional finite environment: $x \in \Omega = [0, L]$.

We assume that $c(x,t)$ is being produced or activated at one boundary ($x = 0$). From there, it diffuses into the environment, where it is inactivated at a rate proportional to its concentration. The concentration of $c(x,t)$ is described by

$$\frac{\partial c(x,t)}{\partial t} = D\frac{\partial^2 c(x,t)}{\partial x^2} - k_- c(x,t). \tag{3.9}$$

We assume that, initially, the concentration is zero everywhere: $c(x,0) = 0$. The production appears as a boundary condition in terms of flux

$$D\frac{\partial c}{\partial x}\bigg|_{x=0} = -k_+.$$

The minus sign corresponds to the fact that the flux is into the domain. The other condition we impose is that there is no flux at the other end of the domain:

$$\frac{\partial c}{\partial x}\bigg|_{x=L} = 0.$$

The solution of this differential equation, written in terms of the steady state ($c_\infty(x)$) and transient ($\tilde{c}(x,t)$), is given by

$$c(x,t) = \underbrace{\frac{k_+\lambda}{D}\frac{\cosh([x-L]/\lambda)}{\sinh(L/\lambda)}}_{c_\infty(x)} + \underbrace{\frac{k_+}{D}\sum_{n=-\infty}^{\infty}\tau_n\cos\left(\frac{n\pi x}{L}\right)e^{-t/\tau_n}}_{\tilde{c}(x,t)}, \tag{3.10}$$

where $\lambda = \sqrt{D/k_-}$ and $\tau_n = 1/[k_- + n^2\pi^2 D/L^2]$. The functions $\cosh(z) = (e^z + e^{-z})/2$ and $\sinh(z) = (e^z - e^{-z})/2$ are the hyperbolic cosine and sine, respectively. The time-dependent spatial profile of this solution is illustrated in figure 3.2.

Although this chapter focuses on the steady-state solution, it is important to keep in mind that, in biology, the transient term may be crucially important (Bergmann et al., 2007).

3.2.2 Controlling the Shape of the Gradient

The parameter λ is known as the *dispersion*. The steady-state spatial gradient of the diffusing species is controlled by the nondimensional parameter

$$\Phi = \frac{L}{\lambda} = \sqrt{\frac{L^2 k_-}{D}},$$

known as the Thiele modulus. We will focus on the concentration at the two ends. First, we look at the end from which the species is being produced or activated ($x = 0$):

$$c_\infty(0) = \frac{k_+\lambda}{D}\coth(\Phi).$$

Then we look at the other end ($x = L$):

$$c_\infty(L) = \frac{k_+\lambda}{D\sinh(\Phi)}.$$

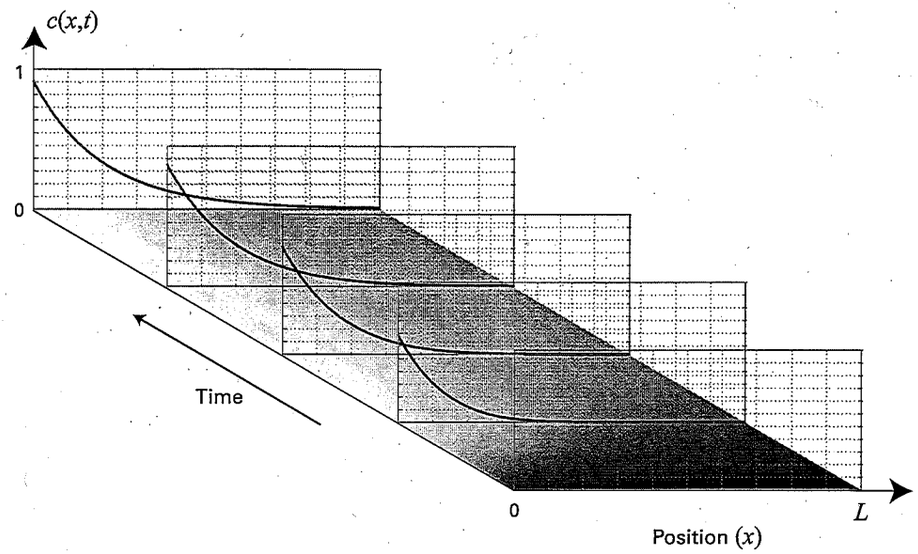

Figure 3.2
Time-dependent solution of equation (3.9), with zero initial condition for a region of length $L = 1$ μm. Coefficients used are $k_- = 1\ s^{-1}$, $D = 10\ \mu m^2/s$, and $k_+ = 1\ \mu M(\mu m\ s)^{-1}$. Shown along the plane is the time-dependent concentration, with darker shades representing lower concentrations. Also shown is the concentration at three intermediate points and at-steady state as a function of the position (x).

Finally, as a measure of the spatial distribution, we look at the gain, defined as the ratio between the two:

$$\frac{c_\infty(0)}{c_\infty(L)} = \cosh(\Phi).$$

These three curves are plotted in figure 3.3 as a function of the Thiele modulus.

Clearly, there are three ways that the Thiele modulus can be regulated: L, k_- and D. We now turn to how each of these can be used in biology to control cell function.

Size and Shape of the Cell

Cells can use the dimension and shape of the environment to regulate the concentration of $c(x,t)$ (Meyers et al., 2006). As the dimension L is increased, two things are apparent. First, the concentration $c_\infty(0)$ is a monotonically decreasing function of L, reaching the asymptotic value of $k_+\lambda/D$ as $L \uparrow \infty$ (figure 3.3a). Hence the larger the environment, the smaller the peak concentration of $c_\infty(x)$, and this is relatively constant once $\Phi \simeq 1$. Consequently, the concentration throughout the region is also lowered. Second, at the other end ($x = L$), $c_\infty(L)$ decreases exponentially for $\Phi \gg 1$. Thus, in addition to the overall level decreasing, the gradient gain increases substantially (figure 3.3b).

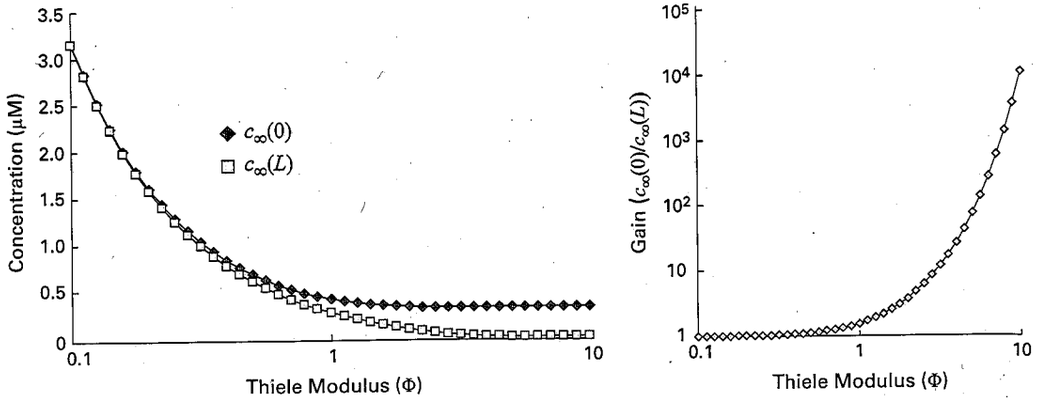

Figure 3.3
Concentration gradient (a) and gain (b) as a function of the Thiele modulus. The coefficients used are $D = 10\ \mu m^2/s$, $k_+ = 1\ \mu M(\mu m\ s)^{-1}$ and $k_- = 1\ s^{-1}$.

This form of control can be used in two ways. First, assume that the environment is growing (for example, a rod-shaped bacterium that is lengthening, or a limb that is growing during development). How does the organism know that it has reached the correct size? One way that has been proposed is through the use of morphogen gradients (Day and Lawrence, 2000). In this case, the source of the morphogen is away from the region of growth. As shown in the model above, as the size of the organism increases, the concentration $c_\infty(x)$ decreases uniformly. Once this reaches a certain threshold, cues stopping growth can be triggered. There is considerable evidence for such a mechanism in wing size determination in *Drosophila* (Hufnagel et al., 2007).

Size can also be used to control the concentration of the diffusing species and related downstream signaling. Consider a situation in which a cell transduces a signal sensed at its membrane into a nuclear signal. This transfer of information takes place by producing an intracellular molecule at the membrane, and allowing it to diffuse toward the nucleus. Figure 3.4 contrasts the signal sensed at the nucleus as a function of cell shape. In the ellipsoidal cell, because the distance between the membrane and the nucleus is smaller, the overall concentration is higher than in the spherical cell. It is clear that the shape of the cell can greatly affect the signal received at the nucleus.

3.2.3 Controlling the Degradation Rate

The degradation rate k_- appears in the numerator of the dispersion λ. Hence, k_-'s effect on determining the shape of the gradient is similar to that of L. The parameter k_- specifies the average lifetime of a molecule. In particular, if we assume that the

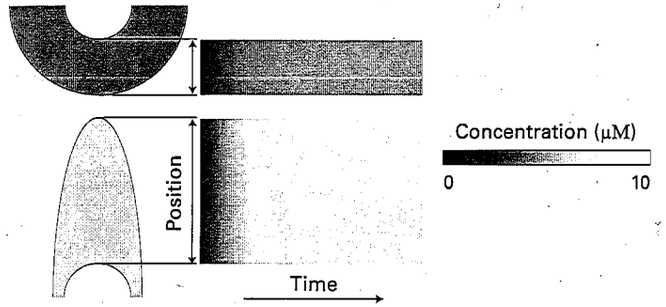

Figure 3.4
Effect of domain shape on concentration of the diffusing species. In this simple model showing only half the domain and the steady-state concentration, a species is released at the cell membrane (*outer circle* or *ellipse*) and diffuses in the domain, having zero flux at the nucleus (*inner circle*). Also shown is the concentration as a function of time along the radial axis. It is clear that the steady-state concentration in the ellipsoidal cell is higher than that of the spherical cell, even though the cell area is the same.

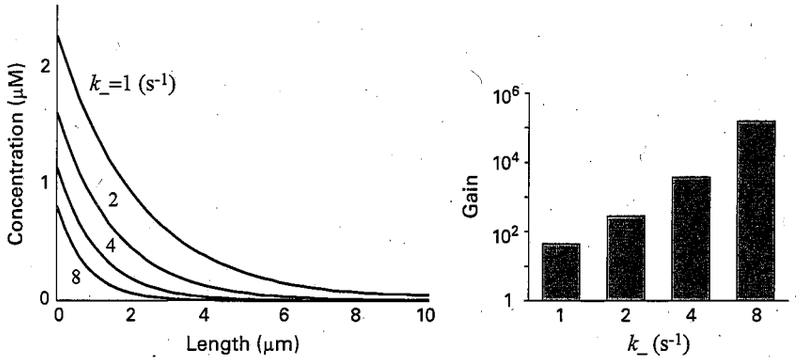

Figure 3.5
Effect of degradation rate on gradient. Concentration along a domain of length $L = 10\ \mu m$ as a function of the degradation rate k_-. Other coefficients are as in figure 3.3.

decay or inactivation of individual molecules is a Poisson process, then the average lifetime $\langle t \rangle = 1/k_-$. In this time frame, the mean-square displacement is given by equation (3.8):

$$\langle x^2 \rangle = 2D\langle t \rangle = \frac{2D}{k_-}.$$

Thus larger values of k_- signify shorter lifetimes over which the molecule diffuses. Thus, fewer activated molecules reach the other end: $x = L$. This translates to fewer molecules throughout the environment, as well as steeper gradients (figure 3.5).

The Ran (Ras-related nuclear protein) system is an example of how k_- is regulated to control the gradient of a diffusible protein (Caudron et al., 2005). Ran is a small GTPase, found in both inactive (RanGDP) and active (RanGTP) forms inside cells, with its activity being dictated by whether it is bound to GDP or GTP. Its spatial regulation follows closely the simple model described above. RanGDP is converted to RanGTP through the action of an enzyme, RCC1 (regulator of chromosome condensation 1), that is found on the surface of the chromatin. Thereafter, RanGTP diffuses into the cytoplasm, where it is hydrolyzed (converted to RanGDP) through the action of a second enzyme, RanGAP (Ran GTPase-activating protein).

Inside the cytoplasm, RanGTP binds to a third molecule, known as importin-β. Through in vitro studies, the compound of RanGTP:Importin-β has been found to be extremely stable: its dissociation rate (k_-) is on the order of 4.5×10^{-4} s^{-1}, meaning that, on average, it stays around for approximately 2,000 seconds. With this lifetime, the dispersion of the RanGTP:Importin-β complex is approximately 165 μm, which is considerably larger than the typical cell dimension.

In live cells, another protein, RanBP1 (Ran Binding Protein 1) helps to break down the RanGTP:Importin-β compound, allowing RanGTP to be hydrolyzed. In the presence of RanBP1, the dissociation rate of RanGTP and importin-β increases about 1,000-fold, making the dispersion length about the radius of the cell. This simple calculation suggests that, in a cell with reduced levels of RanBP1, the abundance of RanGTP:Importin-β would be considerably reduced; this, indeed, has been observed experimentally (Li et al., 2007).

3.2.4 Controlling the Diffusion Coefficient

The third way in which the gradient can be controlled is through the diffusion coefficient. In practice, this can be achieved by changing the local environment in which the molecules are expected to diffuse. Cellular particles have to diffuse in a crowded environment that may have considerable number of physical barriers preventing easy passage. Moreover, the diffusing molecules may interact with other species, hindering their movement. These effects can lead to a greatly reduced effective diffusion coefficient. As an example, the effective diffusion coefficient of a fluorescently tagged morphogen known as Decapentaplegic (Dpp) in the developing fruit fly wing has been measured to be 0.1 $\mu m^2/s$, which is three orders of magnitude less than would be expected according to its size when diffusing freely in water (section 3.6.3).

An interesting and somewhat paradoxical property of regulation through the diffusion coefficient is that, because the concentration of the species near the source increases as the diffusion coefficient is decreased (figure 3.6), it may lead to activation farther away from the source (Lander, 2007). Depending on where the threshold for activation is set, decreased diffusion may lead to a greater portion of the environment being above the threshold. This behavior was seen in a recent model of the Sonic

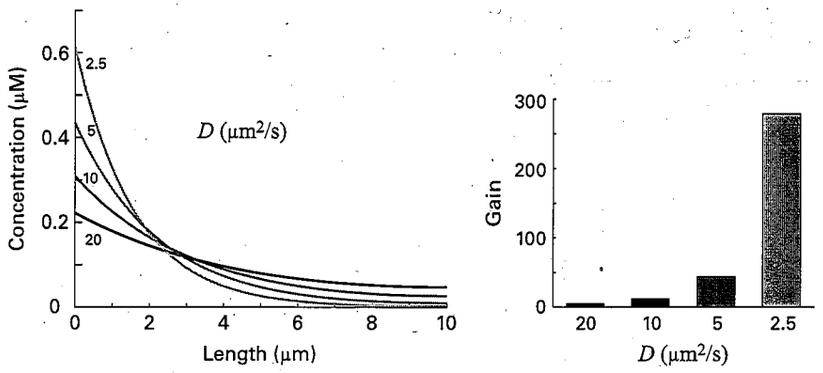

Figure 3.6
Effect of diffusion coefficient. Reducing the diffusion coefficient increases the gradient (gain). Although this reduces the concentration far away from the source, it also increases the concentration near the source.

hedgehog (Shh) gradient that patterns the ventral neural tube of the chick embryo (Saha and Schaffer, 2006).

3.3 Turing Patterns

The concept of the morphogen gradient, though now a well-accepted principle in developmental biology, is not the only model that has been used to account for pattern formation during development. In his influential 1952 paper, Alan Turing proposed that systems could provide the basis for morphogenesis—the formation of shapes in biology. Turing reasoned that, however devoid of shape biological systems might be in their early stages, during development, patterns appeared and that these patterns might be due to an instability of the spatially homogeneous solution. These diffusion-driven bifurcations are now named Turing instabilities. To someone not familiar with this class of systems, the fact that diffusion can destabilize a stable system may be somewhat surprising. After all, alone, diffusion acts to minimize spatial heterogeneities.

The Turing mechanism provides an elegant model of how pattern formation may arise and has been used to account for a large number of patterns seen in biology, from pigmentation patterns in large cats (Liu et al., 2006) to vertebrate limb development (Newman et al., 2008). Because of the lack of experimental data supporting it, and because data from some of the better-studied developmental systems have called its validity into question (Maini et al., 2006), it has not been widely accepted in the biological community. Recently, however, experimental evidence supporting the Turing mechanism has emerged. Thomas Schlake and coworkers identified WNT

and its inhibitor Dickkopf (DKK) as primary determinants of murine hair follicle spacing and confirmed predictions of a WNT/DKK-specific mathematical model based on the Turing mechanism (Sick et al., 2006).

3.3.1 Turing Instabilities in Two-Component Systems

To see how these instabilities arise, we consider a system with two interacting species (say U and V) that are capable of diffusing. The system is described by

$$\frac{\partial}{\partial t}\begin{bmatrix} U(x,t) \\ V(x,t) \end{bmatrix} = \begin{bmatrix} f(U,V) \\ g(U,V) \end{bmatrix} + \begin{bmatrix} D_u \nabla^2 U(x,t) \\ D_v \nabla^2 V(x,t) \end{bmatrix}.$$

We assume that the system has a spatially homogeneous solution with $\overline{U}$ and $\overline{V}$:

$$f(\overline{U},\overline{V}) = 0, \quad \text{and} \quad g(\overline{U},\overline{V}) = 0,$$

with $\nabla^2 \overline{U} = 0$ and $\nabla^2 \overline{V} = 0$. We linearize the system around this equilibrium. Defining

$$u(x,t) = U(x,t) - \overline{U} \quad \text{and} \quad v(x,t) = V(x,t) - \overline{V},$$

we obtain

$$\frac{\partial}{\partial t}\begin{bmatrix} u(x,t) \\ v(x,t) \end{bmatrix} = \underbrace{\begin{bmatrix} a_{11} & a_{12} \\ a_{21} & a_{22} \end{bmatrix}}_{A}\begin{bmatrix} u(x,t) \\ v(x,t) \end{bmatrix} + \underbrace{\begin{bmatrix} D_u & 0 \\ 0 & D_v \end{bmatrix}}_{D}\begin{bmatrix} \nabla^2 u(x,t) \\ \nabla^2 v(x,t) \end{bmatrix}, \tag{3.11}$$

where $\boldsymbol{A}$ is the Jacobian and $\boldsymbol{D}$ is a diagonal matrix describing the species diffusion rates.

We seek conditions under which

1. without diffusion, the spatially homogeneous equilibrium is stable; and
2. with diffusion, it becomes unstable.

The first condition requires that the matrix $\boldsymbol{A}$ be Hurwitz. Because this is a system of two interacting species, we can turn to section 1.4.1 to note that stability is equivalent to the following two inequalities:

$$\text{trace}(\boldsymbol{A}) = a_{11} + a_{22} < 0, \tag{3.12}$$

and

$$\det(\boldsymbol{A}) = a_{11}a_{22} - a_{12}a_{21} > 0. \tag{3.13}$$

We now consider the second condition. We assume that the perturbations about the spatially homogeneous solutions are of the form

$$\begin{bmatrix} u(x,t) \\ v(x,t) \end{bmatrix} = \begin{bmatrix} u_0 \\ v_0 \end{bmatrix} e^{\lambda t} e^{jqx}.$$

(Recall that we use the notation $j = \sqrt{-1}$.) These solutions oscillate in space (with wavelength $q/2\pi$), and their stability is determined by the sign of λ. As we will see later, the size of the spatial domain determines which values of q are admissible. For now, we do not restrict q.

Substituting these solutions into the linear equation (3.11) leads to

$$(\lambda \boldsymbol{I} - \boldsymbol{A} + \boldsymbol{D}q^2)\begin{bmatrix} u_0 \\ v_0 \end{bmatrix} = \boldsymbol{0}.$$

These solutions are unstable if the real part of λ is positive. Thus the system is unstable because of diffusion if the matrix $\boldsymbol{A} - \boldsymbol{D}q^2$ has eigenvalues with positive real part; that is, if

$$\begin{aligned} \text{trace}(\boldsymbol{A} - \boldsymbol{D}q^2) &= a_{11} + a_{22} - q^2(D_u + D_v) \\ &= \text{trace}(\boldsymbol{A}) - q^2(D_u + D_v) > 0, \end{aligned} \tag{3.14}$$

or

$$\begin{aligned} \det(\boldsymbol{A} - \boldsymbol{D}q^2) &= (a_{11} - q^2 D_u)(a_{22} - q^2 D_v) - a_{12}a_{21} \\ &= a_{11}a_{22} - a_{12}a_{21} - q^2(a_{11}D_v + a_{22}D_u) + q^4 D_u D_v \\ &= \det(\boldsymbol{A}) - q^2(a_{11}D_v + a_{22}D_u) + q^4 D_u D_v < 0. \end{aligned} \tag{3.15}$$

We can immediately make several observations.

1. *If the diffusion coefficients are equal ($D_u = D_v = d$), then the homogeneous equilibrium is stable.* To see this, note that

$$\lambda \boldsymbol{I} - \boldsymbol{A} + \boldsymbol{D}q^2 = (\lambda + dq^2)\boldsymbol{I} - \boldsymbol{A}.$$

Thus the eigenvalues of $\boldsymbol{A} - \boldsymbol{D}q^2$ are those of $\boldsymbol{A}$, shifted to the left by $dq^2 > 0$.

2. *Diffusive instabilities can arise only if inequality (3.15) holds.* Because $\text{trace}(\boldsymbol{A}) < 0$, and $q^2(D_u + D_v) > 0$, it is clear that

$$\text{trace}(\boldsymbol{A} - \boldsymbol{D}q^2) = \text{trace}(\boldsymbol{A}) - q^2(D_u + D_v) < 0.$$

This inequality implies that inequality (3.14) cannot hold. Thus, if a diffusive instability exists, then it must be because inequality (3.15) holds.

3. *If the system has a diffusive instability, then the diagonal coefficients of A must have opposite signs, as must the off-diagonal coefficients.* To see why this assertion holds, note that inequality (3.12) requires that at least one of the two diagonal elements be negative. If, however, both $a_{11} < 0$ and $a_{22} < 0$, then

$$-q^2(a_{11}D_v + a_{22}D_u) > 0,$$

and each of the three terms in inequality (3.15) is positive, implying that the inequality cannot hold. It follows that $a_{11}a_{22} < 0$. However, this inequality, along with $\det(A) > 0$, means that

$$a_{12}a_{21} < a_{11}a_{22} < 0.$$

Thus, without loss of generality, we may assume that diffusive instabilities arise only in systems where the Jacobian has one of two sign patterns:

$$A = \begin{bmatrix} + & - \\ + & - \end{bmatrix}, \quad \text{or} \quad A = \begin{bmatrix} + & + \\ - & - \end{bmatrix}. \tag{3.16}$$

4. *If the system has a diffusion-driven instability, then the dispersion of v must be greater than that of u.* We have already established that diffusion-driven instability requires that inequality (3.15) hold. Because both the constant and q^4 terms are positive, however, this means that the q^2 term must be negative:

$$-q^2(a_{11}D_v + a_{22}D_u) < 0.$$

Dividing by $-q^2D_uD_v$, we obtain

$$\underbrace{\frac{a_{11}}{D_u}}_{1/\lambda_u} > \underbrace{\frac{(-a_{22})}{D_v}}_{1/\lambda_v} > 0.$$

Hence $\lambda_v > \lambda_u$, as claimed. Note that the dispersion of species v requires a minus sign because the coefficient $a_{22} < 0$. Normally, this would have been written as $a_{22} = -k_{v,-}$ to match the format of section 3.2.

Condition (3.16) implies that two interacting patterns are possible for a system with diffusion-driven instability. In the first case, species u contributes both to its own production ($a_{11} > 0$) and to that of v ($a_{21} > 0$). Similarly, v negatively regulates both u and v ($a_{12} < 0$ and $a_{22} < 0$, respectively). For this reason, u and v are referred to as the activator and inhibitor, respectively (figure 3.7). Moreover, because the dispersion of v is greater than that of u, activator-inhibitor systems are said to require local enhancement and long-range inhibition.

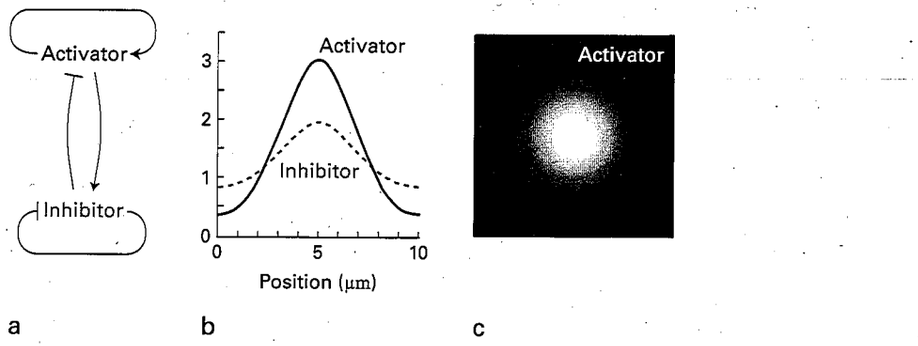

Figure 3.7
Activator-inhibitor system. (a) Activator acts to increase the concentrations of both itself and the inhibitor, whereas the inhibitor acts to decrease the concentration of both. (b) Typical profile for the activator and inhibitor in a one-dimensional problem. (c) Typical profile for the activator in a two-dimensional system. The model used for the latter is that of section 3.4.

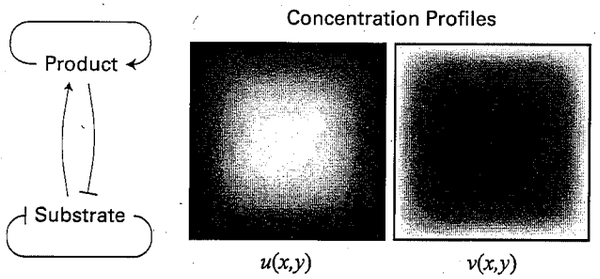

Figure 3.8
Substrate depletion. In these systems, the substrate is needed for the production of the product. As product is formed, substrate is depleted. Shown is the spatially dependent concentration of both the product ($u(x, y)$) and substrate ($v(x, y)$) for the system described in section 3.5.

In the second case, production of u is activated both by its own presence ($a_{11} > 0$) and by the presence of v ($a_{12} > 0$). However, an increase in u reduces the concentration of v ($a_{21} < 0$). In this mechanism, species v can represent a substrate required for the formation of u. As u is formed, the amount of v is depleted; as more substrate is produced, more u can also be produced. For this reason, systems with this type of sign pattern are referred to as substrate-depletion systems (figure 3.8).

We now consider inequality (3.15), a quadratic function of q^2, in greater detail. As stated above, because the coefficients in front of the q^4 and q^0 terms are both positive, the quadratic function can only take negative values if the discriminant is positive:

$$(a_{11}D_v + a_{22}D_u)^2 > 4D_uD_v(a_{11}a_{22} - a_{12}a_{21}).$$

Dividing by $(D_uD_v)^2$ yields

$$\left(\frac{a_{22}}{D_v} + \frac{a_{11}}{D_u}\right)^2 > 4\left(\frac{a_{11}}{D_u}\frac{a_{22}}{D_v} - \frac{a_{12}}{D_u}\frac{a_{21}}{D_v}\right),$$

which is equivalent to

$$\left(\frac{a_{22}}{D_v} - \frac{a_{11}}{D_u}\right)^2 > 4\left|\frac{a_{12}}{D_u}\frac{a_{21}}{D_v}\right| > 0. \tag{3.17}$$

Because $a_{11} > 0$ and $a_{22} < 0$,

$$\frac{a_{22}}{D_v} - \frac{a_{11}}{D_u} = -\left(\left|\frac{a_{22}}{D_v}\right| + \left|\frac{a_{11}}{D_u}\right|\right) < 0.$$

Thus, by taking square roots of equation (3.17), we obtain the inequality

$$\frac{a_{11}}{D_u} - \frac{a_{22}}{D_v} > 2\sqrt{\left|\frac{a_{12}}{D_u}\right|\left|\frac{a_{21}}{D_v}\right|} > 0. \tag{3.18}$$

3.3.2 Effects of Spatial Dimension on the Appearance of a Pattern

If there is no restriction on the spatial parameter q, then inequality (3.18) provides a necessary and sufficient condition for the existence of a Turing instability. In general, however, q cannot be chosen arbitrarily, but is instead constrained by the dimensions of the environment over which the solution evolves.

As an example, consider the case of a finite, one-dimensional domain $\Omega = [0, L]$ with Dirichlet or Neumann boundary conditions. The spatial dimension restricts q to one of the discrete values, known as *wave numbers*:

$$q \in \{q_n\}, \qquad \text{where} \qquad q_n = \frac{2\pi n}{L}.$$

Moreover, the general solution of the linearized equation (3.11) is

$$\begin{bmatrix} u(x,t) \\ v(x,t) \end{bmatrix} = \sum_n \begin{bmatrix} u_{0,n} \\ v_{0,n} \end{bmatrix} e^{\lambda_n t + jq_n x}.$$

The individual modes in this sum are unstable if and only if

$$\det(A) - q_n^2(a_{11}D_v + a_{22}D_u) + q_n^4 D_u D_v < 0$$

for the discrete values of q_n.

As shown in figure 3.9, it may happen that inequality (3.18) holds for some q, but not for the admissible values of q_n. We also see that, as the size of the environment grows, an ever-increasing number of modes can become unstable. This observation fits the general intuition of how spatial patterns may arise during development. It is possible that in a small organism, no discrete mode may satisfy inequality (3.15). As the organism grows, however, a greater number of unstable modes may arise, leading to different patterns. As an example, models have been used to explain the coloration patterns of the growing angelfish *Pomacanthus semicirculatus* (Painter et al., 1999). When young, the fish displays three white stripes on a dark background. As it grows, new stripes develop and insert themselves between the preexisting stripes. The appearance of these extra stripes can be attributed to the extra modes that become unstable.

3.4 Activator-Inhibitor Systems

In 1972, Alfred Gierer and Hans Meinhardt rediscovered that differences in the diffusion properties of interacting species could lead to unstable homogeneous solutions. More important, by developing nonlinear models incorporating local enhancement and long-range inhibition, they moved away from the linear determination of instability that Turing carried out to the development of models that displayed the patterns. Over the years, they have developed a large number of models describing patterns arising in biology (Meinhardt, 1982). Let us consider their original model of an activator-inhibitor system, which was postulated as a means of explaining tentacle formation in hydra (Gierer and Meinhardt, 1972).

The nonlinear system of equations is given by

$$\frac{\partial u}{\partial t} = \frac{\alpha u^2}{v} - \beta u + \epsilon D\frac{\partial^2 u}{\partial x^2},$$

$$\frac{\partial v}{\partial t} = \gamma u^2 - \delta v + D\frac{\partial^2 v}{\partial x^2},$$

where all of the parameters α, β, γ, δ, ϵ, and d are positive constants. The homogeneous solution is given by the pair

$$(\bar{u}, \bar{v}) = \frac{\beta\delta}{\alpha\gamma}\left(1, \frac{\gamma}{\delta}\right)$$

and the associated Jacobian

$$A = \begin{bmatrix} 2\alpha\bar{u}/\bar{v} - \beta & -\alpha\bar{u}^2/\bar{v}^2 \\ 2\gamma\bar{u} & -\delta \end{bmatrix} = \begin{bmatrix} \beta & -\beta^2/\alpha \\ 2\alpha\delta/\beta & -\delta \end{bmatrix}.$$

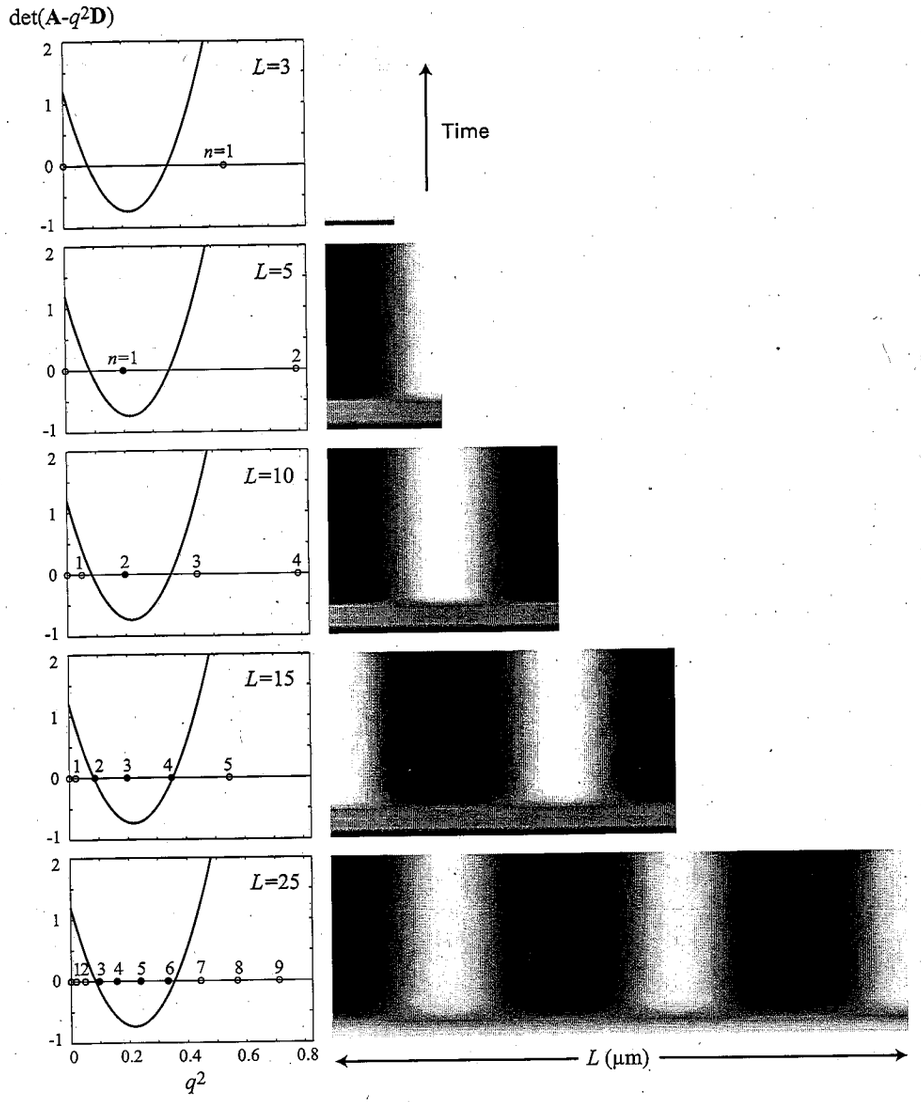

Figure 3.9
Effect of spatial dimension on the existence of instabilities. The spatial dimension specifies the allowable wave numbers that become unstable. The system of figure 3.7 is simulated on a series of one-dimensional domains of different size. In all these cases, the parameters are such that instabilities may arise. Shown is the quadratic term from inequality (3.15). If the length is 3 μm, however, no wave number is unstable; for increasing lengths, different wave numbers become unstable. Which pattern dominates will be determined by the initial conditions and the real value of the wave numbers' eigenvalues.

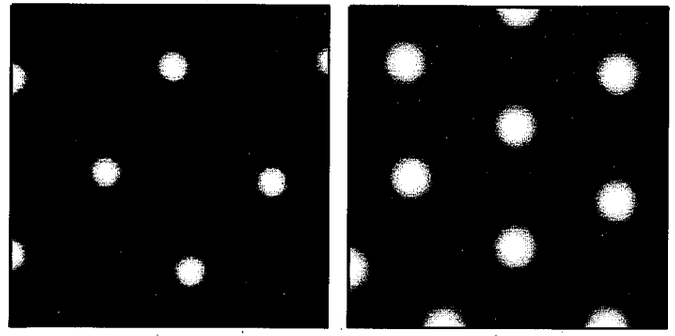

Figure 3.10
Turing instabilities. Shown are different patterns obtained by the activator-inhibitor system described in section 3.4. Parameters used are $\alpha = 1$, $\beta = 1$, $\gamma = 1$, $\delta = 1.1$, $D = 10$, and $\epsilon = 0.1$.

The requirement that $\det(A) = 2\beta\delta > 0$ is satisfied automatically. The second stability requirement: $\text{trace}(A) = \beta - \delta < 0$, is satisfied provided that $\delta > \beta$. From inequality (3.18), for diffusion-driven instabilities to arise, we require that

$$(\beta + \delta\epsilon)^2 > 4\beta\delta\epsilon,$$

which is satisfied provided that

$$\epsilon < (3 - \sqrt{8})\frac{\beta}{\delta} \approx 0.17\frac{\beta}{\delta}.$$

3.5 Substrate Depletion

In equation (3.16), instabilities can also arise from the sign pattern corresponding to a substrate-depletion system. An example of such a system is given by the following set of equations (Barrio et al., 1999):

$$\frac{\partial u}{\partial t} = \alpha u + v + r_1 uv + r_2 uv^2 + \epsilon D\frac{\partial^2 u}{\partial x^2},$$

$$\frac{\partial v}{\partial t} = \gamma u - \beta v - r_1 uv - r_2 uv^2 + D\frac{\partial^2 v}{\partial x^2}.$$

In addition to the linear component, there are two terms that denote exchange from v to u. The two parameters r_1 and r_2 dictate whether the exchange is linear or quadratic in v. Thus the corresponding nonlinearities are either quadratic or cubic.

The homogeneous solutions for this systems are given by

$$v = -\frac{\alpha+\gamma}{1-\beta}u, \qquad \beta \neq 1.$$

By setting $\gamma = -\alpha$, we restrict the steady-state value to the origin: $(u, v) = (0, 0)$. In this case, the Jacobian is

$$A = \begin{bmatrix} \alpha & 1 \\ -\alpha & -\beta \end{bmatrix},$$

which fits the sign pattern. The equilibrium is stable if $\beta > \alpha > 0$ and $\alpha\beta + \gamma < 0$. Inequality (3.18) predicts that diffusion will destabilize the system if

$$\alpha + \epsilon\beta > 2\sqrt{\alpha\epsilon}.$$

Following Liu et al. (2006), we select

$$\alpha = 0.899, \quad \beta = 0.91, \quad D = 6, \quad \epsilon = 0.075, \quad r_1 = 2, \quad \text{and} \quad r_2 = 3.5.$$

A spatially heterogeneous pattern obtained using this system is shown in figure 3.8.

3.6 Determining Diffusion Coefficients

The reaction diffusion equations, together with the initial and boundary conditions specify the system describing the concentration of molecules in the system. To determine the system's evolution requires that we know the correct value of the diffusion coefficient inside living cells. This section describes how diffusion coefficients can be measured.

3.6.1 Fluorescence Recovery after Photobleaching

We first consider the diffusion of molecules that move along the surface of a membrane, which can be that of the cell or an intracellular object, such as the nucleus. Because of this restriction, the molecules diffuse in two dimensions. We are also going to assume that the diffusing species is not interacting or, more likely, that its concentration is at steady state, so the number of molecules is not changing.

The idea behind *fluorescence recovery after photobleaching* (FRAP) is to create in the living cell a discontinuous initial condition in the spatial distribution of the fluorescence of the molecule of interest. This is done by taking advantage of a property of biological fluorophores known as photobleaching. When the fluorescent molecules are exposed to light, they fluoresce, and this response can be detected in the microscope. When the light power from the laser is sufficiently strong, however, irreversible photochemical bleaching of the fluorophore in that region ensues. After this photobleaching, the light and dark molecules diffuse into and out of the initially dark area leading to a blurring of the dark area's boundary (figure 3.11).

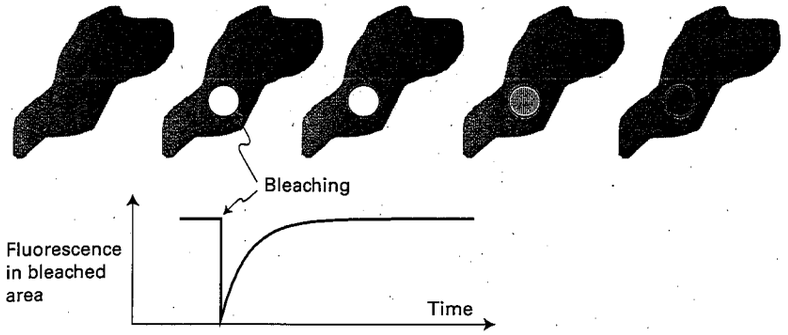

Figure 3.11
Fluorescence recovery after photobleaching. Using a high-powered laser, the fluorescence in a small region (*white circle*) can be eliminated. Diffusion replenishes the area of fluorescent fluorophores; the rate of recovery can be used to measure the diffusion coefficient.

The recovery rates of this brightness can be used to determine the diffusion coefficients (Axelrod et al., 1976). If $c(r, t)$ denotes the concentration of the unbleached fluorophores, then

$$\frac{dc(r,t)}{dt} = -aI(r)c(r,t),$$

where $I(r)$ denotes the intensity of the laser light that induces the photobleaching. Solving this equation leads to the function

$$c(r,t) = c(r,0)\exp[-aI(r)t].$$

Typically, it is assumed that the laser power has a Gaussian profile. For simplicity, however, we assume a perfectly circular profile of radius r_0:

$$I(r) = \begin{cases} P_0/\pi r_0^2, & r < r_0, \\ 0, & r \geq r_0, \end{cases}$$

where P_0 is the total laser power.

In the absence of interactions, equation (3.4) reduces to the simpler diffusion equation

$$\frac{\partial c(\boldsymbol{x},t)}{\partial t} = D\nabla^2 c(\boldsymbol{x},t).$$

Under the assumption that the bleached area is small, the boundary condition is $c(r = \infty) = c_0$, and the initial condition is

$$c(r,0) = \begin{cases} c_0 \exp[-aI(r)T], & r < r_0, \\ c_0, & r \geq r_0, \end{cases}$$

where T is the time over which the laser is used. Integrating over the bleached spot, we define

$$\bar{c}(t) = \int c(r,t)\, \mathrm{d}^2 r.$$

The solution to this diffusion equation leads to an expression describing the fractional recovery:

$$f(t) = \frac{\bar{c}(t) - \bar{c}(0)}{\bar{c}(\infty) - \bar{c}(0)},$$

given by

$$f(t) = 1 - \frac{\tau_D}{t} e^{-2\tau_D/t}[I_0(2\tau_D/t) + I_1(2\tau_D/t)],$$

where I_0 and I_1 are modified Bessel functions and $\tau_D = r^2/4D$ (Soumpasis, 1983). Based on this equation, one way of determining τ_D, and hence D, is to measure $f(t_{1/2}) = 1/2$, which leads (Axelrod et al., 1976) to

$$D \approx 0.224 \frac{r_0^2}{t_{1/2}}.$$

3.6.2 Fluorescence Correlation Spectroscopy

For molecules that are free to diffuse in three dimensions, the preferred technique is *fluorescence correlation spectroscopy*, in which the laser light is focused on an extremely small sample (approximately one femtoliter). Molecules in this volume fluoresce, and the intensity of the emitted light (denoted $I(t)$) is measured and tracked over time. As the molecules diffuse, the measured fluorescence intensity fluctuates. One way of determining the amount of diffusion is to evaluate the normalized autocorrelation function:

$$G(\tau) = \frac{\langle I(t)I(t+\tau)\rangle}{\langle I^2(t)\rangle} - 1.$$

For particles diffusing in three dimensions, the autocorrelation is given (Haustein and Schwille 2007) by

$$G(\tau) = G(0) \frac{1}{1 + \tau/\tau_D} \frac{1}{\sqrt{1 + (r_0^2/z_0^2) \cdot (\tau/\tau_D)}},$$

where r_0 and z_0 describe the radius and height of the volume onto which the laser beam is directed. After fitting experimental data to this equation, the diffusion coefficient can be obtained from

$$D = \frac{r_0^2}{4\tau_D}.$$

3.6.3 The Einstein-Stokes Relationship

Particles subject to Brownian motion in a liquid experience force. In 1905, Einstein used statistical mechanics to demonstrate a relationship between this force and the diffusion coefficient. In particular,

$$D = \mathrm{mob}\, k_B T,$$

where k_B is Boltzmann's constant, T is the absolute temperature, and "mob" refers to the particle's mobility, the ratio between the force applied to the particle and its drift velocity:

$$\mathrm{mob} = \frac{v}{F}.$$

Particles diffusing in a liquid at low Reynolds number, which is the case in biology at the cellular level, are said to be undergoing viscous flow. In this case, the relationship between velocity and the resultant drag force is given by

$$F = \gamma v,$$

where γ is the drag coefficient. For a sphere of radius r, the drag coefficient can be computed as

$$\gamma = 6\pi r \eta,$$

where η is the viscosity of the fluid. For water at room temperature, this equals 8.94×10^{-4} Pa·s. Inside a cell, however, this can be 5–10 times larger (Caudron et al., 2005). Together, this means that

$$D = \frac{k_B T}{6\pi r \eta}, \tag{3.19}$$

which is known as the Einstein-Stokes relationship.

Note that equation (3.19) requires that one know the effective radius of the particle. Although in practice unknown, it can be estimated from the protein's mass by assuming that the molecule is a sphere. From the gene's sequence, the chemical composition is known, and hence the mass of the resultant gene product can be easily calculated. The typical unit of mass used in biochemistry is the dalton, which is defined as one-twelfth the mass of a carbon atom, and equals approximately 1.66×10^{-24} g. The conversion factor used from mass to volume is 0.74 ml/gram (Caudron et al., 2005). For example, the green fluorescent protein (GFP) commonly used to tag proteins in living cells is a 26.9 kDa protein. Thus we estimate that it occupies a volume equal to

$$V \approx (26.9 \times 10^3 \text{ kDa})(1.66 \times 10^{-24} \text{ g})(0.74 \text{ ml/gram})$$

$$\approx 3.3 \times 10^{-23} \text{ ml}$$

$$= 3.3 \times 10^{-8} \ (\mu\text{m})^3.$$

Under the assumption that the protein is a sphere, the radius is

$$r = \left(\frac{3V}{4\pi}\right)^{1/3} \approx 1.99 \text{ nm}.$$

The Einstein-Stokes relationship would predict a diffusion coefficient inside the cell equal to

$$D = \frac{k_B T}{6\pi r \eta} \approx 24.4 \ \mu\text{m}^2/\text{s},$$

at 298 K and assuming a viscosity five times higher than water. By way of comparison, the diffusion coefficient of fluorescent proteins inside living cells has been measured to be 22–25 $\mu\text{m}^2/\text{s}$ (Maertens et al., 2005; Potma et al., 2001).

3.7 Conclusions

This chapter has highlighted the need for including spatial dynamics in models of biochemical reactions. As we saw in sections 3.2 and 3.3, diffusion and transport can make significant differences to the response and even stability of systems. An area where more work is needed is in the use of stochastic methods, such as those presented in chapter 2, for explaining spatial phenomena. Andrews and Bray (2004), Elf and Ehrenberg (2004) and Altschuler et al. (2008) provide some of the first results in this important area.

4 Quantifying Properties of Cell Signaling Cascades

Simone Frey, Olaf Wolkenhauer, and Thomas Millat

Cells use transduction pathways in order to respond to signals from their environment. These pathways are composed of specific biochemical networks, which have a characteristic structural design. In recent years, several mathematical models have been proposed to describe signaling processes. When considering the dynamics of a signal transduction pathway, questions about the magnitude of average activation time or duration of a signal arise. Quantitative measures provide one approach for answering such questions. In this chapter, we analyze features such as the signaling time and signal duration of linear kinase-phosphatase cascades. We apply three commonly used mathematical models to show that one main purpose for the specific design of the MAPK (mitogen-activated protein kinase) cascade structure could be to trigger slow signals of short duration. Thus our results may help to explain the design of a specific pathway structure. Furthermore, we examine the deviations that occur when applying different model approximations to describe the same signaling pathway.

4.1 Why We Need Quantitative Measures of Dynamic Properties

The functioning of cells requires the transfer of information between and within cells. The transmission of signals is realized through interacting proteins, groups of which are organized into signaling pathways. Because signal processing and cellular responses are highly dynamic biological processes, the investigation of steady-state behavior is not sufficient to characterize them. As reported in recent publications, changes in the temporal profile of a stimulus can result in very different cellular processes. In PC12 cells, for example, the duration of signaling through extracellular signal-regulated kinases (ERKs) may result in proliferation or in differentiation. The two hormones EGF (epidermal growth factor) and NGF (nerve growth factor) use the same pathway to trigger either process. Stimulation with EGF results in transient ERK phosphorylation, which causes proliferation, whereas stimulation with NGF